

Central Collisions of Charged Dust Particles in a Plasma

U. Konopka and L. Ratke

DLR-Institut für Raumsimulation, Linder Höhe, 51147 Köln, Germany

H. M. Thomas

Max-Planck-Institut für extraterrestrische Physik, 85740 Garching, Germany

(Received 25 February 1997)

Elastic dust particle particle interaction in an rf plasma provides a charge measurement method independent of the knowledge of plasma parameters. Assuming a screened Coulomb potential surrounding each particle with a constant charge at fixed plasma conditions, the charge and the screening length can be calculated from the trajectories of two colliding particles. With this method, we determine the charge and screening length of dust particles in the sheath of an rf discharge. The method can also be used to determine plasma parameters taking the dust particles as local probes. [S0031-9007(97)03864-7]

PACS numbers: 52.25.Vy, 52.65.Cc, 52.90.+z

One of the most interesting aspects of the physical behavior of dust particles in a plasma is the charging effect [1–4]. The charge is influenced by the plasma conditions, and the charged particles themselves change the plasma in their neighborhood. The experimental determination of the charge on particles and the screening length is rather difficult and often leads only to rough estimates or depends on assumptions on plasma parameters like the ion density [5]. Therefore theoretical descriptions of effects that are influenced by charged dust particles rely on estimates or assumptions on the charge [6–10].

We propose here a new approach to the charging problem using central collision experiments of charged dust particles. Their trajectories are mainly determined by the electrical potential around each particle. From the trajectories the relative velocity and the center-to-center distance of the two particles are extracted. Assuming a simple Coulomb potential around each particle we can determine a lower boundary and for a screened Coulomb potential a more realistic value for the charge. These experiments allow one to determine the dust charge and the screening length simultaneously for typical plasma conditions, especially those used in plasma crystal experiments [11–18], where the particles are levitated in the plasma sheath.

In addition, this method should also be useful to measure the charge and screening length in the so-called “gaseous phase” of a plasma crystal by evaluation of single collision events between “crystal” particles.

In combination with the charge measurement methods from Melzer *et al.* [5] or equivalent methods, where the charge determination depends on an assumption of a plasma parameter, the dust particle can be used as a probe to determine plasma parameters, for example, the ion density, or, in combination with the levitation height, the electrical potential in the plasma sheath region.

In a collision of two charged particles, each particle can be treated as a probe in the field of its counterpart. If \mathbf{E}_1

and \mathbf{E}_2 designate the electrical fields exerted by particle 1 on particle 2 and vice versa (Fig. 1), Newton’s law leads to the force equations,

$$\mathbf{F}_1 = m_1 \ddot{\mathbf{x}}_1 = Q_1 \mathbf{E}_2, \quad (1)$$

$$\mathbf{F}_2 = m_2 \ddot{\mathbf{x}}_2 = Q_2 \mathbf{E}_1. \quad (2)$$

If both particles have the same mass $m = m_1 = m_2$ and charge $Q = Q_1 = Q_2$ during the complete collision event, the force difference can be written as

$$m \ddot{\mathbf{d}} = Q(\mathbf{E}_1 - \mathbf{E}_2), \quad (3)$$

where $\mathbf{d} = \mathbf{x}_2 - \mathbf{x}_1$ is the distance between the two particles.

Assuming a screened Coulomb potential around each particle for small horizontal particle velocities (some mm/s)

$$\Phi(r) = \frac{Q}{4\pi\epsilon_0} \frac{e^{-r/\lambda}}{r}, \quad (4)$$

with r as the distance from the center of the charged grain and λ the screening length, Eq. (3) can be rewritten as

$$\ddot{\mathbf{d}} = \frac{2Q}{m} \frac{\partial \Phi(r)}{\partial r} \Big|_{r=d} = \frac{Q^2}{2\pi\epsilon_0 m} \frac{(\lambda + d)e^{-d/\lambda}}{\lambda d^2}. \quad (5)$$

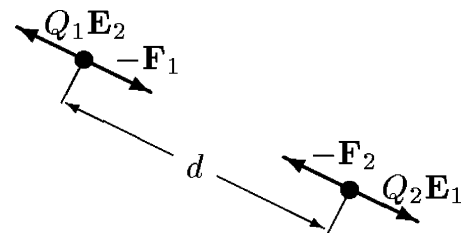


FIG. 1. Sketch of the collision process of two charged particles.

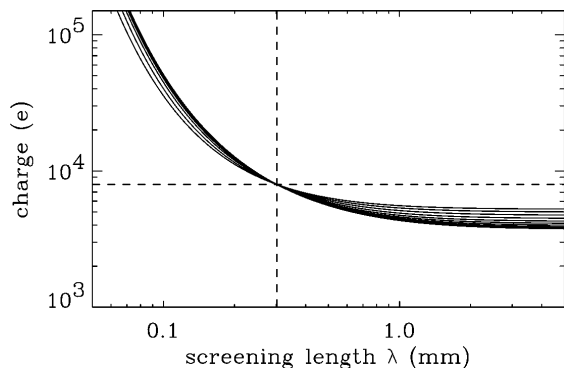


FIG. 2. Calculation of the charge using Eq. (8) by varying the screening length λ in an ideal Coulomb collision. Each curve represents one set of distances and relative velocities. The charge for the simulation was set to 8000 electron charges and the screening length to 0.3 mm.

Equation (4) is only applicable if during a collision event the smallest distance between the particles is larger than the screening length since otherwise the deformation of the ion cloud must be taken into account. Substituting $A = 2\pi\epsilon_0 m \lambda^3 / Q^2$ and $y = d/\lambda$ this equation transforms into the differential equation

$$Ay^2\ddot{y} - ye^{-y} - e^{-y} = 0. \tag{6}$$

Integration leads to the relative velocity \dot{y} ,

$$\dot{y}^2(t) = \frac{2}{A} \left(\frac{e^{-y(t_0)}}{y(t_0)} - \frac{e^{-y(t)}}{y(t)} \right) + \dot{y}^2(t_0), \tag{7}$$

where t_0 and t are time variables. From this equation we calculate the charge using the measurable quantities (1) the relative velocities $\dot{d}(t)$ and $\dot{d}(t_0)$ and (2) the distances $d(t)$ and $d(t_0)$ for two different times t and t_0 ,

$$|Q| = \left(\frac{\pi\epsilon_0 m [\dot{d}(t_0)^2 - \dot{d}(t)^2]}{[e^{-d(t)/\lambda}/d(t)] - [e^{-d(t_0)/\lambda}/d(t_0)]} \right)^{1/2}. \tag{8}$$

Since generally both Q and λ are unknown, the following procedure allows one to find reliable values for both

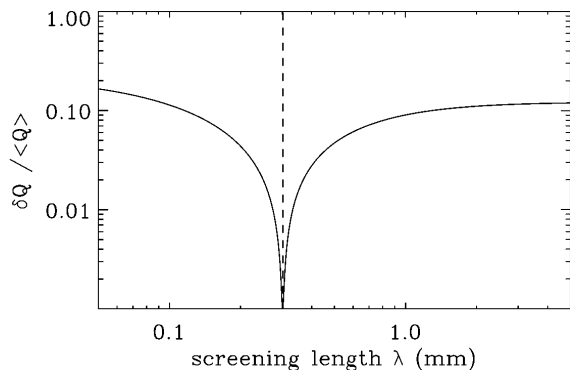


FIG. 3. Relative deviation $\delta Q / \langle Q \rangle$ of the calculated charge as displayed in Fig. 2 dependent on the screening length λ for the simulated Coulomb collision in Fig. 2. The minimum value indicates the best fit of the screening length.

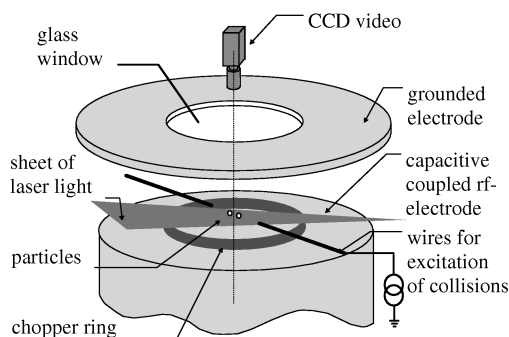


FIG. 4. Sketch of the experimental setup.

concurrently. We use a large set of distances and relative velocity measurements to calculate the charge for a wide range of the screening length and then find that λ for which the calculated relative deviation of the evaluated charges $\delta Q / \langle Q \rangle$ is a minimum (δQ is the standard deviation of Q for a fixed λ). A demonstration of this procedure is shown in Fig. 2. There we simulated a collision of two particles with a screened Coulomb potential ($Q = -8000e$, $\lambda = 0.3$ mm). Taking ten sets of velocities and distances along the trajectories ($d(t_m), d(t_n); \dot{d}(t_m), \dot{d}(t_n)$) Eq. (8) can be evaluated varying the screening length. As expected the relative deviation of the charge, shown in Fig. 3, has its minimum very close to the prescribed screening value.

The experiments were made in an rf-discharge chamber, the so-called GEC RF reference cell. The plasma glows between two electrodes separated by a distance of 3 cm. The lower electrode is capacitively coupled to the rf voltage and the upper one is grounded (Fig. 4). A glass window is built into the upper electrode enabling the observation of the dust particles without influencing the

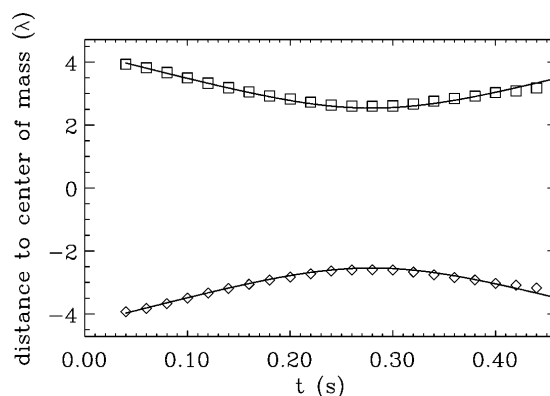


FIG. 5. The particle positions for a typical collision event at a pressure of 2.31 Pa are displayed as a function of time in units of the measured screening length $\lambda = 0.17$ mm relative to the position of the center of mass. Particle one is displayed in the upper part of the figure. The solid lines are trajectories for a simulated collision with $Q = -17000e$, $\lambda = 0.17$ mm, and the special boundary conditions $d_0 = -2.8$ mm/s and $\dot{d}_0 = 1.35$ mm/s.

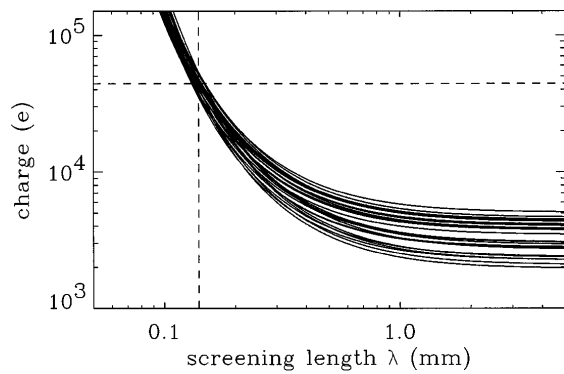


FIG. 6. Calculation of the charge using Eq. (8) in dependency of an assumed screening length λ for a typical collision experiment. Each curve represents one set of distances and relative velocities.

homogeneity of the plasma. A small hole in the center of the glass window is used to inject particles between the two electrodes. The charged particles are levitated in the plasma sheath due to the dc self-bias at the lower electrode. They are illuminated by a sheet of laser light parallel to the electrodes. A copper ring with an inner diameter of 4 cm and a height of 2 mm leads to a small disturbance of the electrical field near the electrode, which helps to keep the dust particles in the center. In addition two wires with a diameter of 2 mm are mounted horizontally inside the chamber. They are located 0.5 cm above the lower electrode pointing to its center from opposite directions. The gap between their ends is 1.6 cm (see Fig. 4). Both wire potentials are floating, but a dc voltage can be applied in a range between 0.0 up to 16.0 V. For an applied positive voltage the two particles move from the center of the chamber to the wires, thus increasing their distance. The elastic collision is triggered if the voltage is switched off, such that the potentials on the wires are floating again. Then the particles are accelerated towards the center above the lower electrode, which leads to a collision event. The acceleration towards the center is

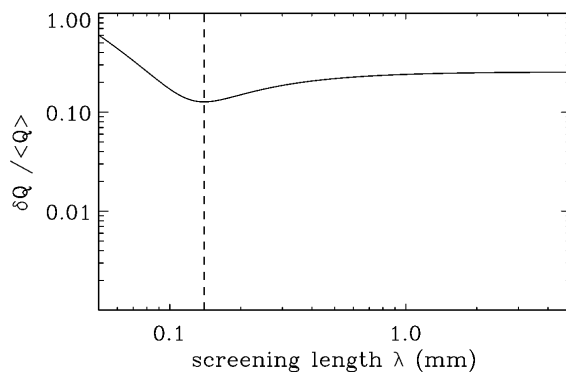


FIG. 7. Relative deviation $\delta Q / \langle Q \rangle$ of the calculated charge as displayed in Fig. 6 as a function of an assumed screening length λ for a typical collision experiment. The minimum value indicates the best fit of the screening length.

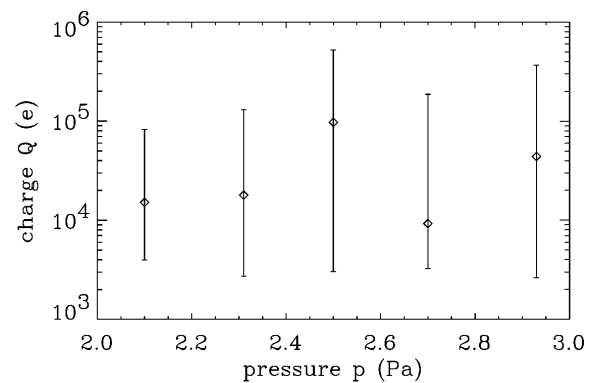


FIG. 8. Evaluated charge depending on the neutral gas pressure for a forward (reflected) rf power of 4.0 (1.0) W and particle size of $6.9 \pm 0.2 \mu\text{m}$ assuming a screened potential surrounding each particle.

induced by the local inhomogeneity of the electrical field close to the copper ring and influences therefore the particle motion only at larger distances from the center of the electrode. This inhomogeneity is negligible in the collision area. A typical collision event is shown in Fig. 5.

The experiments were made with argon gas at low pressures between 2.0 and 3.0 Pa to avoid an influence of the neutral gas friction. The particles used for the collision experiments were monodisperse melamine formaldehyde spheres with a diameter of $6.9 \pm 0.2 \mu\text{m}$ and a density of 1500 kg/m^3 . The induced forward (reflected) rf power was measured to be 4.0 (1.0) W. The charge is calculated for screening lengths in the range from 0.050 to 5.000 mm for each pressure. For all collision processes observed the total momentum was calculated and only those events evaluated with respect to charge and screening length whose total momentum was conserved. A typical result of an experiment performed at a gas pressure of 2.93 Pa is shown in Fig. 6 (this figure compares to the simulated process shown in Fig. 2). The relative deviation of the charge has a minimum at $\lambda = 0.14 \text{ mm}$ as seen in Fig. 7. For this screening length we

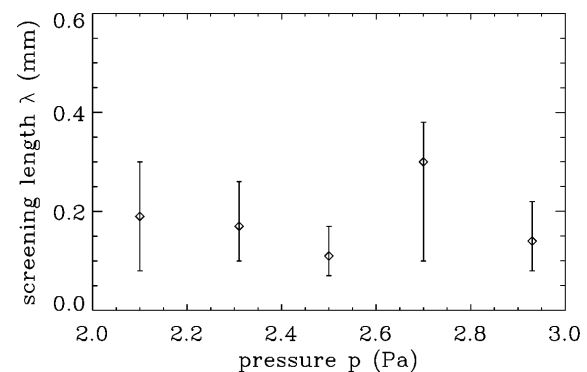


FIG. 9. Evaluated screening length of the potential surrounding a single particle depending on the neutral gas pressure for a forward (reflected) rf power of 4.0 (1.0) W and particle size of $6.9 \pm 0.2 \mu\text{m}$.

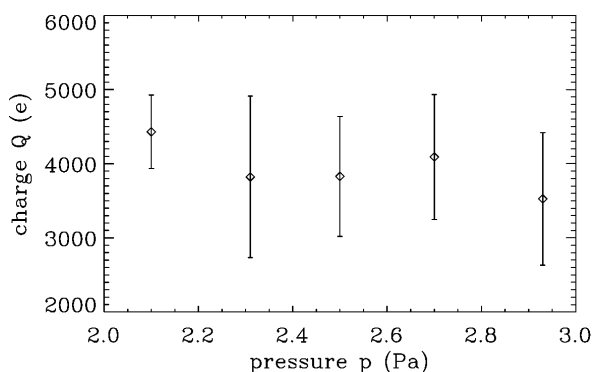


FIG. 10. Evaluated charge depending on the neutral gas pressure for a forward (reflected) rf power of 4.0 (1.0) W and particle size of $6.9 \pm 0.2 \mu\text{m}$ assuming that the potential surrounding a single particle is unscreened.

calculated the average charge on the particle by Eq. (8) to 43 000 electron charges. The uncertainties of the charge and screening length can be calculated from the standard deviation over all intersections of the functions $Q(\lambda)$ calculated for every set of velocities and distance measurements. All results for a screened Coulomb potential are shown in Figs. 8 and 9. The approximation of an unscreened Coulomb potential around each particle leads to charge values of a few thousand electron charges as displayed in Fig. 10. The error bars are the standard deviation for the charge in the limit of $\lambda \rightarrow \infty$. The large error bars are mainly a result of the uncertainties in the determination of the trajectories due to the limited time and spatial resolution of the camera system. The measured values for the charge are to an order of magnitude in good agreement with other experimental charge evaluations [18]. In order to compare the screening length obtained by our new method with the electron or ion Debye length we performed measurements with a Langmuir probe [19]. At a pressure of 2.4 Pa we measured a plasma density of $n = 5 \times 10^{15} \text{ m}^{-3}$ and an electron energy in the range of 2 to 3 eV. The electron and ion Debye lengths were determined as $\lambda_{De} = 0.15, \dots, 0.18 \text{ mm}$ and $\lambda_{Di} = 0.017 \text{ mm}$ with a thermal energy of the ion of $kT_i = 0.025 \text{ eV}$. The screening lengths measured with the collision events correspond to the electron Debye length, in accordance with exper-

imental results obtained by Peters *et al.* [20] and theoretical considerations from Hamaguchi and Farouki [21].

For further investigations it should be possible to obtain more information about the plasma surrounding a particle by similar experiments, if the measurement of their positions and velocities could be improved, for example, by using a high speed high resolution camera system. Research along this line is currently in progress.

We would like to thank M. Zuzic for helpful discussions.

-
- [1] C. K. Goertz, *Rev. Geophys.* **27**, 271 (1989).
 - [2] E. Whipple, *Rep. Prog. Phys.* **44**, 1197 (1981).
 - [3] S. Choi and M. Kushner, *Appl. Phys. Lett.* **62**, 2197 (1993).
 - [4] J. Goree, *Plasma Sources Sci. Technol.* **3**, 400 (1994).
 - [5] A. Melzer, T. Trottenberg, and A. Piel, *Phys. Lett. A* **191**, 301 (1994).
 - [6] F. Melandsø, *Phys. Plasmas* **3**, 3890 (1996).
 - [7] V. A. Schweigert *et al.*, *Phys. Rev. E* **54**, 4155 (1996).
 - [8] H. Ikezi, *Phys. Fluids* **29**, 1764 (1986).
 - [9] X. Wang and A. Bhattacharjee, *Phys. Plasmas* **3**, 1189 (1996).
 - [10] P. K. Shukla and N. N. Rao, *Phys. Plasmas* **3**, 1770 (1996).
 - [11] H. M. Thomas *et al.*, *Phys. Rev. Lett.* **73**, 652 (1994).
 - [12] J. Chu and L. I., *Phys. Rev. Lett.* **72**, 4009 (1994).
 - [13] Y. Hayashi and K. Tachibana, *Jpn. J. Appl. Phys.* **33**, L804 (1994).
 - [14] H. M. Thomas and G. E. Morfill, *Nature (London)* **379**, 806 (1996).
 - [15] M. Zuzic, H. M. Thomas, and G. E. Morfill, *J. Vac. Sci. Technol. A* **14**, 496 (1996).
 - [16] G. E. Morfill and H. M. Thomas, *J. Vac. Sci. Technol. A* **14**, 490 (1996).
 - [17] L. I., W.-T. Juan, C.-H. Chiang, and J. H. Chu, *Science* **272**, 1626 (1996).
 - [18] A. Melzer, A. Homann, and A. Piel, *Phys. Rev. E* **53**, 2757 (1996).
 - [19] J. D. Swift and M. R. J. Schwar, *Electrical Probes for Plasma Diagnostics* (ILIFFE, London, 1970).
 - [20] S. Peters, A. Homann, A. Melzer, and A. Piel, *Phys. Lett. A* **223**, 389 (1996).
 - [21] S. Hamaguchi and R. T. Farouki, *Phys. Plasmas* **1**, 2110 (1994).